Simulation and Measurement-based X-parameter Models for Power Amplifiers with Envelope Tracking

Haedong Jang[1], Andrew Zai[2], Tibault Reveyrand[3], Patrick Roblin[1], Zoya Popovic[2], and David E. Root[4]

[1]The Ohio State University, Columbus, OH

[2]University of Colorado, Boulder, CO

[3]XLIM-UMR CNRS, Limoges Cedex, France

[4]Agilent Technologies, Santa Rosa, CA

Abstract —Static X-parameter (XP) models for RF power amplifiers (PAs), derived from both simulations and nonlinear vector network analyzer (NVNA) measurements, are investigated for the prediction of PA performance under dynamic signal conditions such as in envelope tracking (ET). The instantaneous AM-AM, AM-PM and PAE predictions of XP models extracted from simulation are compared under ET dynamic signal conditions to two types of circuit models using envelope simulation. An XP PA model is extracted for a peak 8W GaN class-F^{-1} ET PA from NVNA measurements with automated bias control. By applying a constant gain shaping table derived from the XP model to the drain supply voltage, the average PAE is improved from 40% to 57% for 3.84 MHz WCDMA signals at 2.14 GHz compared to fixed drain bias operation.

Index Terms — X-parameters, envelope tracking, loadpull, power amplifiers, supply modulation.

I. INTRODUCTION

High data rate communication requires spectrally efficient complex modulation schemes such as WCDMA and LTE, resulting in signals with high peak to average power ratios (PAPR). These dynamic signals significantly degrade the average PA efficiency when operated at a fixed bias condition. The envelope tracking (ET) architecture has shown significant improvement of the average efficiency by dynamically adjusting PA supply voltages according to look-up tables (LUT), or shaping tables, that specify mappings from input RF time-varying envelopes to drain control signals on the PA [1].

Nonlinear characterization and modeling of the transistor that can predict PA performance under varying bias and load is needed for more complex transmitters, such as those that employ envelope tracking [2]. A simplified ET block diagram is shown in Fig. 1 with a nonlinear RF PA that can be viewed as a three-port device, with the third port being the supply input. Most transistor and PA models are not designed with dynamic bias taken into account. Assuming the device under test (DUT) is quasi-static to the varying supply voltages and the envelope tracker is ideal, the common PA performance figure of merits (FOMs) such as AM-AM, AM-PM and PAE, can be determined using the conventional static

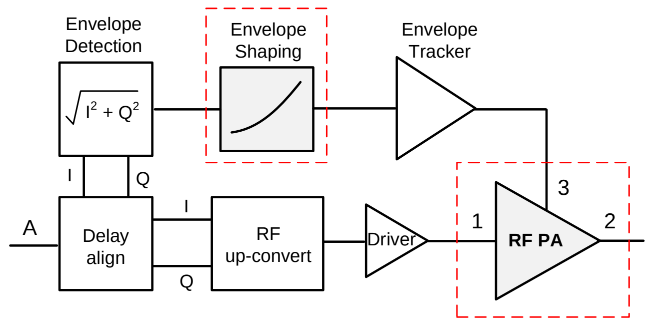

Fig. 1. Simplified ET-PA system block diagram with a nonlinear three-port RF PA.

characterization at multiple supply voltages. The goal of this work is to develop a model for this application that is easy to extract from simulations and standard measurements for the shaping table design, and validate that it gives good estimates of the PA performance under dynamic bias operation.

In this work, bias dependent static X-parameter (XP) behavioral models [3][4] are developed from simulations and from nonlinear vector network analyzer (NVNA) measurements to model the nonlinear RF PA for use under dynamic signal operation with supply modulators. Properties of the bias dependent static X-parameter models are summarized in section II. In section III, the FOMs of the static model are compared to those of circuit models using dynamic input signals. In section IV, a static XP model is extracted from an S-band class-F^{-1} GaN PA. A shaping table is designed from the model and used to define dynamic drain control signals to improve efficiency. The intended FOMs based on the static model are measured under the dynamic ET condition using the supply modulator from [1].

Furthermore, the performance prediction of a model with varying loads is critical for LUT designs and PA performance optimizations under antenna mismatch condition [5]. The load dependency prediction of the XP models including harmonic loads [6] is validated by comparing the XP model, extracted from NVNA measurements in 50Ω, to time-domain loadpull data from an independent measurement system. Then the

978-1-4673-2141-9/13/$31.00 ©2013 IEEE

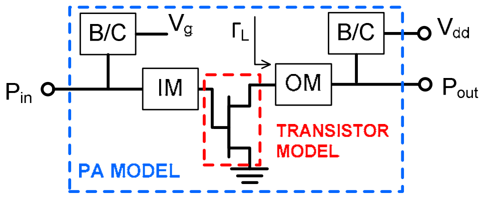

Fig. 2. Two different XP models were extracted from a circuit model. (1) An XP model was extracted from the entire PA (blue) (2): XP model was extracted only of the transistor (red) and then embedded in matching (IM, OM) and bias circuitry (B/C).

effect of the load variation on the shaping table design is presented.

II. Bias Dependent XP Model

In the frequency domain, the scattered m^{th} harmonic component at port p is expressed by (1) at static RF conditions at controlled DC bias conditions [3][4][6]. The model is characterized over a large set of drain voltages and a wide range of RF powers of the input driving signal. For time-varying bias and modulated RF input signals, the XP models approximate the PA behavior through the quasi-static approximation by evaluating (1) with time-varying arguments when simulated in the envelope domain.

$$\begin{aligned} B_{p,m} &= X^{(F)}_{p,m}\left(DC,|A_{11}|\right)P^{m} \\ &+\sum X^{(S)}_{p,m,q,n}\left(DC,|A_{11}|\right)P^{m-n}A_{q,n} \\ &+\sum X^{(T)}_{p,m,q,n}\left(DC,|A_{11}|\right)P^{m+n}A^{*}_{q,n} \end{aligned} \tag{1}$$

The additional S and T terms linearly estimate the effect of the incident n^{th} harmonic and its conjugate from the port q to the scattered harmonic of interest, effectively predicting the PA performance with varying load nearby the load where the X-parameters were extracted. This has been demonstrated to be accurate for power amplifier applications where perturbations are relatively small compared to the large driving signal [6]. Extraction tones were applied in the measurements for the identification of those terms. The amplitude of the tones was selected 16 dB lower than the main large tone for proper linear approximation. Evenly distributed four phases were used to acquire the conjugate component. Phases of respective harmonic components are normalized relative to the input large signal by the P term.

III. Simulation-based XP Modeling

In this section, two types of static XP behavioral models are generated from PA models in the Agilent ADS simulator using continuous wave (CW) RF excitation at different static drain bias conditions. Then the XP models and the underlying circuit models are compared under modulated RF signal conditions, first under fixed bias conditions and second under dynamic supply modulation conditions applied using a drain-control LUT based on the XP model.

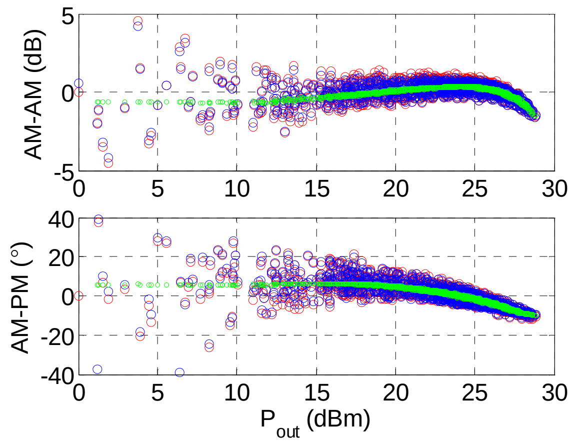

Fig. 3. AM-AM, AM-PM simulation results for LTE UL signals at fixed bias conditions. The XP model for the whole amplifier (green), XP model of bare transistor (blue) embedded in the matching and bias circuitry of the PA, the circuit model (red).

The PA circuit model is based on a silicon MOSFET transistor model, biased at V_{gs}=1.75 V for class AB operation with 27.9 dBm output power at 1 dB compression. XP models were extracted in two different cases, as shown in Fig. 2. In case (1), the entire matched amplifier, including the transistor model and bias and matching networks, is converted into an XP model. The input power was swept from -10 to 26 dBm to model the PA in saturated operation. The drain voltage was swept from 1.5 to 6 V for ET design resulting in a three terminal nonlinear model. In case (2), the bare transistor model was converted into a load-dependent XP model, and the circuitry for bias and matching are embedded around the XP transistor model. The input power range and loads used for the XP extraction of the bare transistor are different from that of the whole PA. The input power range for the bare transistor XP extraction was from -20 to -1 dBm. Instead of 50Ω, the

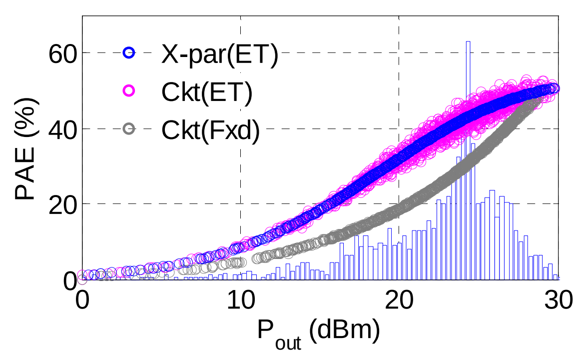

Fig. 4. Simulation results for an LTE signal and a CMOS PA under ET operation compared to fixed bias condition operation. Both XP model and circuit model show improved efficiency. The XP model estimates the ET performance improvement over static bias very closely to that of the circuit model. A histogram of the LTE signals is shown for reference.

978-1-4673-2141-9/13/$31.00 ©2013 IEEE

load seen from the transistor, $\Gamma_L(\omega) = 0.79\angle 157.6$, was estimated from the circuit model and applied to the drain of the transistor. Also, the load was swept around the selected point with 0.1 step for the magnitude and 3° for the phase.

The dynamic AM-AM, AM-PM envelope simulation results using LTE uplink signals at fixed bias conditions for the XP models and the underlying circuit models are shown in Fig. 3. The signals were generated using 16 QAM modulations with 5 MHz bandwidth. When the whole PA circuit model was replaced by the XP model as in case 1 (green), no gain and phase spreading is observed for the time-varying signals as with the detailed circuit model (red). However, the average gain and phase, which corresponds to the static nonlinearity of the XP model, is well-represented. When only the transistor was replaced by the XP model, case 2 (blue), the instantaneous signal follows well the results of the circuit model (red). The spreading can be concluded to come primarily from the bias and matching networks in this example. It should be noted that only the input signal induced dynamic effects are present with the fixed bias while both input and supply induced dynamics are present under ET.

A LUT for ET operation of the PA was designed using static gain curves as functions of drain voltage predicted by the XP model of the entire PA. The envelope simulation results of the XP model under ET operation and fixed bias conditions with the above LTE signals are compared to the circuit model in Fig. 4. The average PAE simulated, using the XP model, was 43.3% (ET) compared to 31.5% (fixed bias) which is very close to the results obtained from the circuit model of 42.4% (ET) compared to 31.7% (fixed bias) for the same average output power of 24 dBm for a fair comparison. ADS examples showing envelope tracking may be downloaded from [7].

IV. Measurement Based X-parameter Extraction and Experimental Validation

X-parameters of a class-F^{-1} GaN HEMT 8-W PA [8], based on a TriQuint TGF2023-02 transistor, were measured at 2.14GHz in CW mode using an NVNA. The NVNA automatically characterized and generated an X-parameter model as a function of drain voltage and RF power. The X-parameters were measured in a nominally 50Ω system. Five harmonics of the scattered waves, magnitudes and phases, were measured. The drain voltage varied over the range 12 to 30 V. Auxiliary amplifiers were used for both input and output to boost the source power. External couplers were used with additional attenuators considering peak powers. The input power was swept from 0 to 25 dBm. The extraction tones were selected to be 16 dB lower than the peak operating power for both input and output with 4 phases.

In order to verify the XP model extracted from the NVNA frequency domain measurement instrument, the DUT was measured at various bias and load conditions on an independent time domain loadpull system - a VTD (now Agilent) sampler-based SWAP-X402. In Fig. 5, gain and PAE versus output power curves are compared at two different loads, specified in the caption, at a fixed drain bias of 28V.

The XP model, generated from measurements into fixed impedance of nominally 50Ω was able to track the significant load-dependent performance characteristics of the amplifier, without the need for a load tuner. Given the fidelity of the load-dependent XP model predictions, additional load variation effects on the LUT design were investigated. Fig. 6 illustrates just how much the corresponding LUT for constant gain ET operation depends on load, for four different complex reflection coefficients of $|\Gamma| \leq 0.1$.

The PA performance under ET conditions, based on the static XP model, was measured using a WCDMA signal as shown in Fig. 7. The test signal, with duration of 1 ms and 3.84 MHz bandwidth, was generated and the LUT was applied to the signal to generate the drain supply control signal. This control signal was fed to the supply modulator using an arbitrary waveform generator. The original WCDMA signal was up-converted by an ESG and fed to the input of the PA through a linear driver amplifier. In-phase and quadrature phase data from input and output ports were recorded. The operation, at fixed bias conditions of 26 V, 28 V and 30 V,

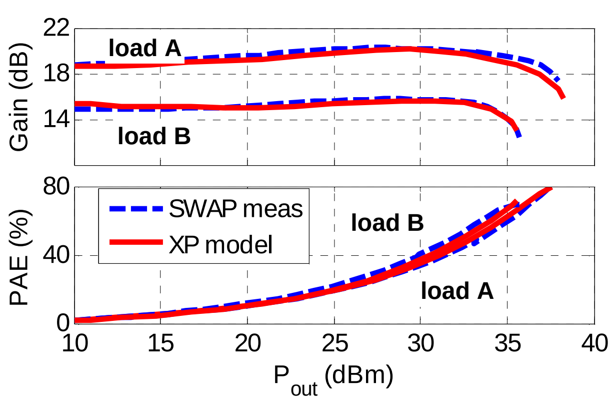

Fig. 5. PA gain and PAE versus power at two different loads at fixed V_{dd}=28 V. Predictions from the NVNA measurement-based XP model (red), verification by measured results (blue) using a sampler-based SWAP time-domain loadpull system. Load A: $\Gamma_L(\omega) = 0.173\angle 11.2°$. Load B: $\Gamma_L(\omega) 0.293\angle 178.8°$).

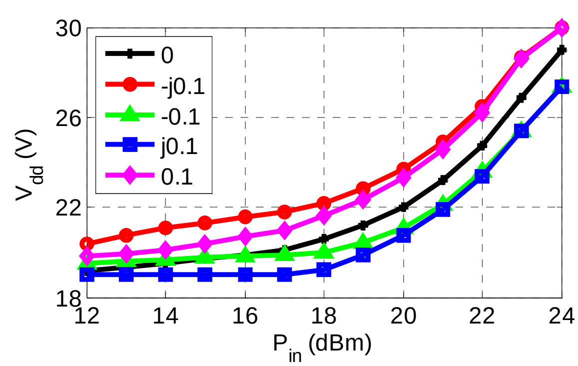

Fig. 6. The constant-gain LUT dependence on fundamental load, computed from the measured and validated XP model, is quite significant, even for reflection coefficient magnitudes as small as 0.1.

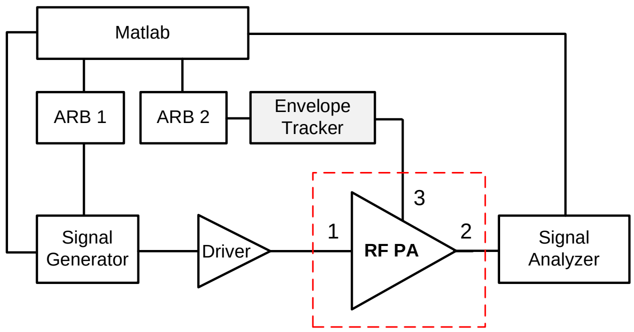

Fig. 7. The baseband WCDMA signal was generated by arbitrary signal generator (ARB) 1 and fed to a RF signal generator. ARB 2 generates shaped drain control signal and fed to the envelope tracker. A signal analyzer recorded 1 ms long baseband complex data.

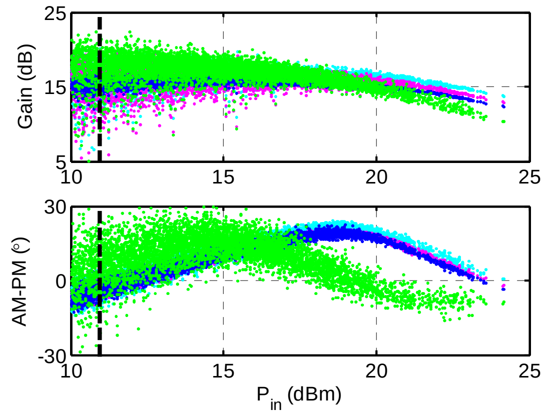

Fig. 8. The measured ET (green) gain and phase variations are compared to the fixed bias (cyan: 30V, pink: 28 V, blue: 26V) conditions with WCDMA down link signal. The supply voltage does not vary for input power levels below the black dashed line.

was also measured for comparison. The signal sources were synchronized by sharing a 10 MHz reference.

The measured average PAE under ET condition excluding the supply modulator was 57.8 % with 31.28 dBm output power while the PAE of the three fixed bias cases showed 40.3 % in average with 30.6 dBm average output power. The measured average drain voltage during the ET operation was 21V, which is well below the fixed bias conditions. The designed average output power was 28.8 dBm.

As shown in Fig. 8, ET operation showed more gain compression above 18 dBm than the fixed bias conditions. The AM-PM characteristics under ET operation show wider spreading. We expect that some of this spreading can be attributed to increased memory effects under dynamic biasing different from the assumption of ideal linear operation. A systematic characterization of the supply modulator could be developed to consider the imperfect modulator characteristics into the design.

V. Conclusion

Simulation-based and measurement-based frequency domain static XP models were investigated specifically for envelope tracking power amplifiers. The envelope simulation and measurement results show good quantitative agreement for the static nonlinearity of the PA versus power and drain voltage, and also as a function of load. A new result is the load-sensitivity of the lookup table predicted by the XP model that was independently validated by time-domain loadpull measurements. It is expected that the static X-parameter based end-to-end measurement-based design flow should meet the commercial specifications, at least for amplifiers not exhibiting significant long-term memory effects.

As future work, limitations of the quasi-static approach can be explored by treating the RFPA as a mixer, with the bias pin treated as a second large signal incommensurate with respect to the RF input tone. Another approach would use the dynamic extensions of X-parameters [9] applied to both the RF and the supply ports.

Acknowledgement

This work was supported by a Grassroots grant from Agilent Technologies and in part by ONR under the DARPA MPC Program N00014-11-1-0931. The authors thank A. Howard, J. Horn, R. Biernacki, M. Marcu, P. Cain, A. Cognata, and J. Xu for support and valuable discussions.

References

[1] J. Hoversten, S. Schafer, M. Roberg, M. Norris, D. Maksimovic, and Z. Poppovic, “Co-design of PA, supply, and signal processing for linear supply-modulated RF transmitter,” *IEEE Trans. Microwave Theory & Tech.*, vol. 60, no. 6, June 2012.

[2] P.M. Asbeck. H. Kobayashi, M. Iwamoto, G. Hanington, S. Nam, L.E. Larson, “Augmented behavioral characterization for modeling the nonlinear response of power amplifiers,” *IEEE MTT-S Intl Microwave Symp. Dig.*, 2002

[3] J. Verspecht, and D.E. Root, “Polyharmonic distortion modeling,” *IEEE Microwave Magazine*, vol. 7, no. 3, June 2006.

[4] D. E. Root, J. Verspecht, D. Sharrit, J. Wood, and A. Cognata, “Broad-band, poly-harmonic behavioral models from fast automated simulations and large-signal vectorial network measurements,” *IEEE Trans. Microwave Theory & Tech.*, vol. 53, no. 11, November 2005. pp. 3656-3664

[5] R. Paul, L. Sankey, L. Corradini, Z. Popovic, and D. Maksimovic, “Power management of wideband code division multiple access RF power amplifiers with antenna mismatch,” *IEEE Trans. on Power Electronics*, Vol. 4, No. 4, Apr. 2010

[6] J. Horn, D. E. Root, and G. Simpson, “GaN device modeling with X-parameters,” *IEEE CSICS* Oct. 2010.

[7] http://edocs.soco.agilent.com/display/eesofkcads/Applying+envelenv+tracking+to+Improve+Efficiency

[8] M. Roberg, J. Hoversten, and Z. Popovic, “GaN HEMT PA with over 84% power added efficiency,” *Electronics Letters*, Vol. 46, No. 23, Nov. 2010

[9] J. Verspecht, J. Horn, L. Betts, D. Gunyan, C. Gillease and D.E. Root, “Extension of X-parameters to include long-term dynamic memory effects,” *IEEE MTT-S Int. Micro. Symp. Dig.* June 2009